# Exploration of Ionic Modification in Dual-Layer Hollow Fiber Membranes for Long-Term High-Performance Protein Separation

**Yi Li and Sim Chuan Soh**
Dept. of Chemical and Biomolecular Engineering, National University of Singapore, Singapore 119260, Singapore

**Tai-Shung Chung**
Dept. of Chemical and Biomolecular Engineering, National University of Singapore, Singapore 119260, Singapore, and Singapore-MIT Alliance, National University of Singapore, Singapore 119260, Singapore

**Sui Yung Chan**
Dept. of Pharmacy, National University of Singapore, Singapore 119260, Singapore

*DOI 10.1002/aic.11671*
*Published online December 17, 2008 in Wiley InterScience (www.interscience.wiley.com).*

*Two types of ionic modification approaches (i.e., sulfonation and triethylamination) were applied with the aid of dual-layer hollow fiber technology in this work to fine tune the pore size and pore size distribution, introduce the electrostatic interaction, and reduce membrane fouling for long-term high-performance protein separation. A binary protein mixture comprising bovine serum albumin (BSA) and hemoglobin (Hb) was separated in this work. The sulfonated fiber exhibits an improved BSA/Hb separation factor at pH = 6.8 compared with as-spun fibers but at the expense of BSA sieving coefficient. On the other hand, the triethylaminated fiber reveals the best and most durable separation performance at pH = 4.8. Its BSA/Hb separation factor is maintained above 80 for 4 days and maximum BSA sieving coefficient reaches 33%. Therefore, this study documents that an intelligent combination of both size-exclusion and electrostatic interaction can synergistically enhance protein separation performance in both purity and concentration.* © 2008 American Institute of Chemical Engineers *AIChE J,* 55: 321–330, 2009
*Keywords: dual-layer hollow fiber membranes, ionic modification, protein separation, size-exclusion, electrostatic interaction*

## Introduction

Proteins are composed of numerous amino acids and the sequence of amino acids in each protein is unique to that protein; therefore, each protein has its own unique three-dimensional shape or native conformation.[1] Proteins are essential parts of organisms and participate in every process within cells. For example, some proteins are enzymes that catalyze biochemical reactions and are vital to metabolism; some proteins have structural or mechanical functions that maintain the cell shape; and other proteins are important in cell signaling, immune responses, cell adhesion, the cell cycle, and so on. As a result, proteins have attracted much attention to comprehend the biochemical mechanisms of

Correspondence concerning this article should be addressed to T.-S. Chung at chencts@nus.edu.sg.

disease, and hence develop drugs with an improved safety profile and a greater probability of clinical trial success.[2] Considering the presence of a large number of impurities, pyrogens, and viruses, an inevitable issue on the separation and purification of proteins must be addressed to gain a comprehensive understanding of protein function and regulation.[3] The U.S. market for protein separation systems is estimated to be valued at almost U$3.0 billion in 2006 and is expected to cross the U$5.0 billion by the year 2011.[4]

It is well known that the protein separation and purification are an arduous task because of the complexity of proteins themselves and their biological environments. To obtain high-purity proteins, many separation techniques have been developed in terms of different properties of proteins, which include precipitation, packed bed chromatography, electrodialysis, electrophoresis, membrane chromatography, and ultrafiltration (UF). Among them, the membrane-based technique such as UF may be a potentially attractive process for the separation and purification of proteins because of its lower capital cost, space compactness, and steady-state operation, which allow an efficient transfer to the large-scale operation.[5] The membrane filtration segment for protein separation in the U.S. market is valued at U$538 million in year 2006 with an estimated growth of 10.8% and is predicted to grow to U$898 million in year 2011.[4]

UF is a variety of membrane filtration in which hydrostatic pressure forces a liquid against a semipermeable membrane. UF membranes typically have pore sizes in the range of 1–100 $\times$ $10^{-9}$ m (1–100 nm) and have been used widely for the concentration, diafiltration, clarification, and fractionation of biomolecules.[6] A previous study[7] documented that protein separation was best obtained for size-exclusion UF membranes if the ratio of their molecular weights (MWs) exceeded 7 as it is not trivial to fabricate UF membranes with a narrow pore size distribution through the phase-inversion method. Nevertheless, it is known that the MW ratio of proteins in mixtures is generally less than 5; therefore, new separation mechanisms to achieve better separation by using the UF technique, such as the electrostatic interaction[8,9] or the affinity interaction,[10,11] have been explored.

Zydney and coworkers have developed the charged UF system and demonstrated that a high-performance protein separation could still be achieved via the electrostatic interaction with small differences in their MWs.[8,9,12,13] This is due to the fact that proteins are known to be electrically neutral at their isoelectric points (pI) and have positive or negative charges at environments with lower or higher pH values, respectively; therefore, the protein transport through charged UF membranes is not only a function of pore sizes of membranes but is also strongly affected by electrostatic interaction.[9,12] Regrettably, the high performance of UF membranes is not easily maintained over time as significant fouling occurs after the process commences.[14–16] Although membrane fouling is a very complicated process, many investigations have shown that an increment in membrane hydrophilicity will inevitably inhibit protein adsorption and deposition, thereby significantly reducing membrane fouling.[17–19]

Therefore, the ionic modification was applied with the aid of dual-layer hollow fiber technology in this work to tune the pore size and pore size distribution, introduce the electrostatic interaction, and reduce membrane fouling for long-term high-performance protein separation. Polyethersulfone (PES) was chosen as the polymer material and two kinds of ionic modification approaches (i.e., sulfonation and triethylamination) were used in the PES membrane. The purpose of employing the dual-layer hollow fiber configuration was to utilize the porous PES inner layer to provide the enough supporting strength for the modified PES outer layer (i.e., functional layer) so that the developed membranes could be run in protein permeation tests. These developed membranes were characterized in terms of scanning electron microscopy (SEM) and neutral solute permeation experiments. Their separation performance for a bovine serum albumin (BSA)-hemoglobin (Hb) binary mixture was measured by an ultraviolet (UV)–visible spectrophotometer.

## Experimental

### *Materials*

A commercial Radel® A PES was obtained from Solvay Advanced Polymers L.L.C., GA, and was dried at 120°C overnight under vacuum before use. *N*-methyl-2-pyrrolidone (NMP), methanol, ethanol, diethylene glycol (DG), glycerol, 37 wt % aqueous solution of hydrochloric acid (HCl), 37 wt % aqueous solution of formaldehyde, zinc chloride ($ZnCl_2$), sodium sulfite ($Na_2SO_3$), and triethylamine all were purchased from Merck. Polyethylene glycol (PEG) from Merck-Schuchardt and polyethylene oxide (PEO) from Sigma-Aldrich with different MWs from 2 to 100 kDa were used as neutral solutes to measure the pore size and pore size distribution of dual-layer hollow fiber membranes developed in this work. Disodium hydrogen phosphate ($Na_2HPO_4$), potassium dihydrogen phosphate ($KH_2PO_4$), acetic acid ($CH_3COOH$), and sodium acetate ($CH_3COONa$) were provided by Aldrich for the preparation of protein buffer solutions with pH values of 4.8 and 6.8. The proteins BSA and Hb were bought from Sigma-Aldrich. The MW and pI value of BSA are 66 kDa and 4.8, respectively; whereas the MW and pI value of Hb are 65 kDa and 6.8, respectively. All these chemicals were of reagent grade and used as received.

### *Preparation of dual-layer hollow fiber membranes*

The dual-layer hollow fiber membranes were fabricated by a coextrusion technique using a dual-layer spinneret as depicted in related literatures.[20–22] The detailed dope compositions and spinning conditions/parameters are summarized in Table 1. The dried polymer powder was dispersed slowly into a chilled solvent and the homogenous polymer dope solutions were achieved under a continuous and vigorous stir for 1 or 2 days. The flow rates of the bore fluid and both polymer dope solutions were controlled by three ISCO pumps during the spinning.

After the spinning, the as-spun dual-layer hollow fibers were rinsed in a clean water bath for 3 days to remove the residue solvent, and then carried out two posttreatment protocols without further drying. One was to dip the hollow fibers in a 50 wt % glycerol aqueous solution for 48 h and dry them in air at ambient temperature for the neutral solute and protein permeation experiments. The other was to directly dry the hollow fibers using a freeze dryer with a model of

**Table 1. The Spinning Conditions for Dual-Layer PES Hollow Fiber Membranes**

| ID | A | B | C | D | E |
|---|---|---|---|---|---|
| Outer-layer dope composition | PES/NMP/DG (23/42/35 wt %) | | | | |
| Inner-layer dope composition | PES/NMP/DG (19/43/38 wt %) | | | | |
| Bore fluid composition | NMP/water (86/14 wt %) | | | | |
| Out-layer dope flow rate (ml/min) | 0.6 | | | | |
| Inner-layer dope flow rate (ml/min) | 2 | | | | |
| Bore fluid flow rate (ml/min) | 0.8 | | | | |
| Air gap (cm) | 0 | 0 | 0 | 2 | 5 |
| Take-up rate (cm/min) (*under free fall) | 327* | 1070 | 1624 | 848* | 1292* |
| External coagulant | Methanol | | | | |
| Spinning temperature (°C) | 25 | | | | |
| Coagulation bath temperature (°C) | 25 | | | | |

Modulyo D from Thermo Electron Corporation for the morphological observation by SEM.

### *Module fabrication and ionic modification*

Two modules for each hollow fiber sample were made for the ionic modification and the permeation experiment, wherein each module comprised 10 fibers with an effective length of around 0.16 m (16 cm) per fiber. Based on the work done by Yang and Lin,[23] two ionic modification methods, namely sulfonation and triethylamination, were developed in this work. First, the chloromethylation of PES hollow fiber membranes was completed by circulating the reaction solution comprising 37 wt % aqueous solution of HCl, 37 wt % aqueous solution of formaldehyde and $ZnCl_2$ along the shell side of modules at 40°C and $1.01 \times 10^5$ Pa (1 atm) for 3 h. Second, to obtain anionic PES fibers (i.e., negative charges), the chloromethylated PES was sulfonated by circulating a mixture of $Na_2SO_3$, ethanol, and deionized (DI) water at 40°C and $1.01 \times 10^5$ Pa (1 atm) for 3 h, whereas to achieve cationic PES fibers (i.e., positive charges), the chloromethylated PES was triethylaminated by circulating a mixture of triethylamine, ethanol, and DI water at 40°C and $1.01 \times 10^5$ Pa (1 atm) for 3 h. Finally, all modified modules were washed with DI water for 1 day to remove the unreacted chemicals. The reaction equations for chloromethylation, sulfonation, and triethylamination are listed as follows:

$$\text{Chloromethylation}: \quad -C_6H_4- + HCHO + HCl \xrightarrow{ZnCl_2} -C_6H_3(CH_2Cl)- + H_2O \qquad (1)$$

$$\text{Sulfonation}: \quad -C_6H_3(CH_2Cl)- + Na_2SO_3 \rightarrow -C_6H_3(CH_2SO_3^-Na^+) + Na^+ + Cl^- \qquad (2)$$

$$\text{Triethylamination}: \quad -C_6H_3(CH_2Cl)- + (C_2H_5)_3N \rightarrow -C_6H_3(CH_2N^+(C_2H_5)_3Cl^-)- \qquad (3)$$

### *Characterizations*

The morphology of dual-layer hollow fiber membranes was observed by SEM on a JEOL JSM-5600LV and JSM-6700F as a function of spinning conditions. Membrane samples were prepared in liquid nitrogen.[24] After mounting the specimens on the stub by using the double-sided conductive carbon adhesive tape, the specimens were stored under vacuum. All samples were sputter coated with platinum of 2–3 $\times 10^{-8}$ m (200–300 Å) in thickness using JEOL JFC-1200 ion sputtering device before testing.

The ion-exchange capacity (IEC) of modified hollow fibers was determined by ion-exchange titration.[23] For the sulfonated hollow fibers, the sulfonic groups were first regenerated by circulating 1 M HCl solution along the shell side of modules at 1 atm for 1 h. Second, they were washed thoroughly with DI water to remove unreacted protons. Third, their shell side was circulated with a 10 wt % NaCl solution at 1 atm for 1 h. Finally, this salt solution was titrated with a 0.01 M NaOH solution to the end point using phenolphthalein as the indicator. The chemical scheme is expressed as follows:

$$\text{Regeneration}: \quad -C_6H_3(CH_2SO_3^-Na^+) + H^+ \text{ (in excess)} \rightarrow -C_6H_3(CH_2SO_3^-H^+) + Na^+ \qquad (4)$$

$$\text{Ion exchange}: \quad -C_6H_3(CH_2SO_3^-H^+) + Na^+ \text{ (in excess)} \rightarrow -C_6H_3(CH_2SO_3^-Na^+) + H^+ \qquad (5)$$

$$\text{Titration}: \quad OH^- + H^+ \rightarrow H_2O \qquad (6)$$

The pore size and pore size distribution of dual-layer hollow fiber membranes were characterized by the neutral solute permeation experiment. PEG and PEO with different MWs were used as neutral solutes to prepare a series of feed solutions with a concentration of 0.2 kg/m$^3$ (0.2 g/l). The concentrations of the feed and permeate solutions were determined by a total organic carbon analyzer (Shimadzu ASI-5000A) during the experimental running. The single solute rejection was calculated by the following equation:

$$R = (1 - C_p/C_f) * 100\% \qquad (7)$$

where $C_p$ and $C_f$ are the single solute concentrations in the permeate and feed solutions (ppm), respectively. The solute rejection results as a function of MWs were further used to estimate the mean pore size and the pore size distribution of membranes.[25,26]

### *Protein separation performance measurements*

The feed solution was pumped into the shell side of fibers (i.e., the selective surface) and the permeate solution exited from the lumen side of fibers, thus forming a cross-flow filtration mode. Except collecting the feed and permeate samples at intervals for the measurement of concentrations, both retentate and permeate solutions were recycled back to the feed tank to keep the concentration of feed solution constant during the whole experimental running. The temperature of feed solution in all experiments was maintained at 18°C by a cooling coil inside the feed tank; the transmembrane pressure was held at $1.01 \times 10^5$ Pa (1 atm), and the feed velocity tangent to the outer surface of fibers was controlled at around 0.78 m/s by adjusting the back pressure valves and bypass valves to minimize the effect of concentration polarization (Reynolds number, Re $\approx$ 5000).

Each module was first subjected to the pure water permeation experiment to remove the glycerol and measure the pure water flux. The normalized pure water permeability [PWP, l/(m$^2$-bar-h)] was calculated by the following equation:

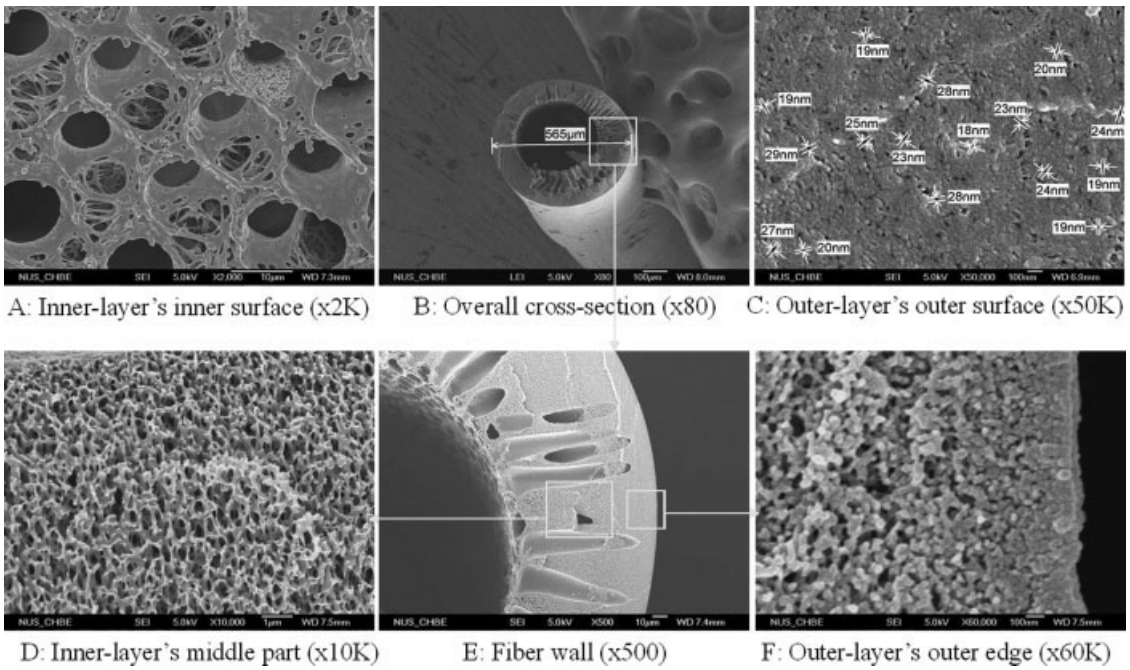


**Figure 1. SEM images of typical morphology of dual-layer PES hollow fiber membranes (fiber B with an air gap of 0 cm and take up rate of 1070 cm/min).**

$$\mathrm{PWP} = Q/(A * \Delta P) \tag{8}$$

where $Q$ is the water permeation rate (l/h), $A$ denotes the effective membrane filtration area ($m^2$), and $\Delta P$ means the transmembrane pressure (bar).

After the pure water permeation experiment, the feed was changed from DI water to a BSA–Hb protein buffer solution (0.1 $kg/m^3$: 0.1 $kg/m^3$) and circulated for 1–5 days to test the protein separation performance of dual-layer hollow fiber samples at pH = 4.8 or 6.8. The protein concentrations in both feed and permeate solutions were determined by an UV–visible spectrophotometer (Biochrom Libra S32). The detailed calculation method has been described in other works[27–29]; therefore, it is not necessary to duplicate it herein. To express the separation performance of dual-layer hollow fiber membranes for the BSA–Hb mixture, the separation factor is defined as follows:

$$\alpha_{\mathrm{BSA/Hb}} = \left(\frac{C_{\mathrm{BSA}}}{C_{\mathrm{Hb}}}\right)_{\mathrm{permeate}} \Bigg/ \left(\frac{C_{\mathrm{BSA}}}{C_{\mathrm{Hb}}}\right)_{\mathrm{feed}} \tag{9}$$

where $C_{\mathrm{BSA}}$ is the BSA concentration ($kg/m^3$), $C_{\mathrm{Hb}}$ means the Hb concentration ($kg/m^3$), and the subscripts permeate and feed represent the solutions in the permeate and feed sides, respectively.

## Results and Discussion

### *Morphology of as-spun dual-layer PES hollow fiber membranes*

Figure 1 shows a typical morphology of the as-spun dual-layer PES hollow fiber membrane, wherein fiber B is used as an example in this study. Its outer diameter is $5.65 \times 10^{-4}$ m (565 $\mu$m) in Figure 1B. Because the same PES, solvent NMP and nonsolvent DG are used in both layers in spite of their different concentrations, it significantly enhances the interfacial diffusion as pointed out in our previous work.[22] Consequently, a delamination-free structure between the inner and outer layers is observed in Figure 1E. In addition, the bulk (Figure 1D) and the inner surface (Figure 1A) of the inner layer as a supporting layer are fully porous, whereas the outer edge (Figure 1F) and the outer surface of the outer layer (Figure 1C) as a selective layer have the much smaller pores in size.

A comparison of different dual-layer PES hollow fiber membranes in their outer-layer's outer surface is illustrated in Figure 2 because the pore size and pore size distribution on the outer surface (i.e., the selective skin) are one of determinant parameters for UF membranes in protein separation. Obviously, the pore size decreases monotonously with an increment in take up rate from 327 to 1624 cm/min, whereas an increase in air gap from 0 to 2 cm reduces the pore size but a further increase in air gap from 2 to 5 cm causes no apparent effect on the pore size. This observation demonstrates that gravity as well as other external work-induced elongation stresses may influence the macromolecular packing and membrane morphology during the spinning, thus affecting the porosity, pore size, and pore size distribution,[30–32] which will be helpful to understand the separation performance of different as-spun dual-layer hollow fiber membranes in the next section.

### *Protein separation performance of as-spun dual-layer PES hollow fiber membranes*

The evolution of BSA/Hb separation factor as a function of time for different as-spun dual-layer PES hollow fiber membranes at pH = 6.8 is illustrated in the left column of

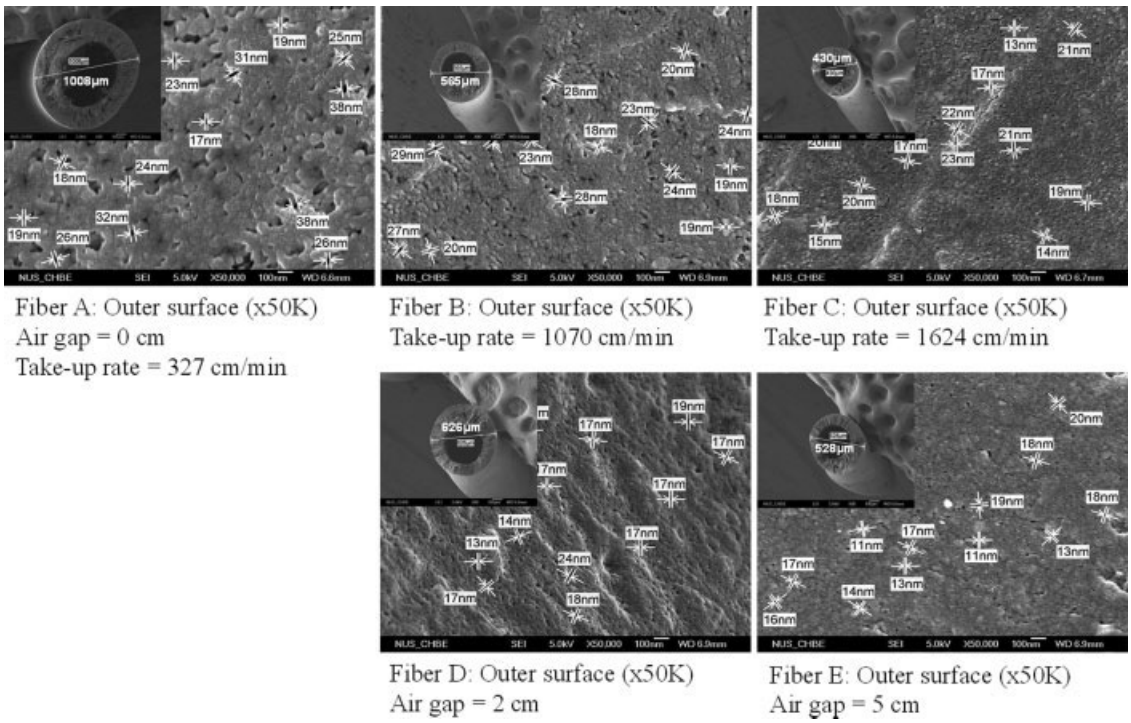


**Figure 2. Comparison of SEM images of outer layer's outer surface of different dual-layer PES hollow fiber membranes (inlet: overall cross-sectional profile).**

Figure 3. Their order of separation performance is fiber C > fiber B > fiber A with the effect of take-up rates and fiber D > fiber E > fiber A with the effect of air gaps, which seems to follow the changing trend in pore sizes as shown qualitatively in SEM images of Figure 2.

To quantitatively correlate the pore size and protein separation performance, a neutral solute permeation experiment was carried out to measure the pore size and pore size distribution of different dual-layer hollow fiber membranes. Their PWP, mean pore size (the geometric mean diameter of a solute with

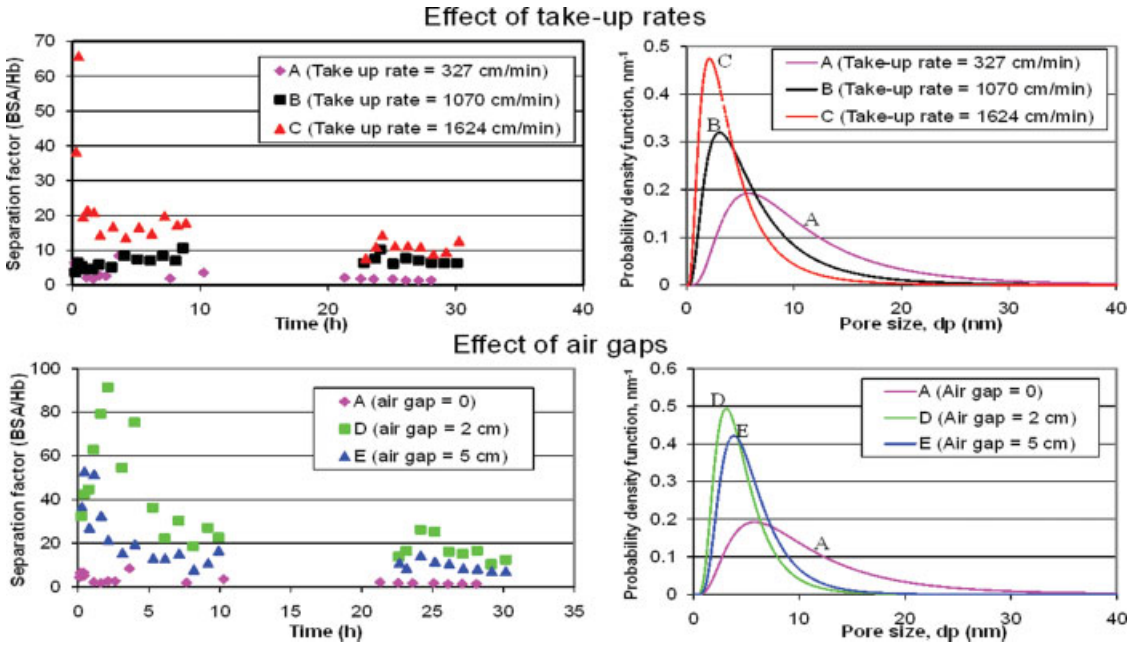


**Figure 3. Evolution of BSA/Hb separation factor over time (left column) and probability density function curves (right column) for different as-spun dual-layer PES hollow fiber membranes.**

[Color figure can be viewed in the online issue, which is available at www.interscience.wiley.com.]

**Table 2. Comparison of Various Parameters of Different Dual-Layer Hollow Fiber Membranes on the Pore Size Distribution Calculated from Neutral Solute Permeation Experiments**

| Fiber ID | Modification Status | PWP (l(m$^2$-bar-h)) | Mean Pore Size, $\mu_p$ (nm) | Standard Deviation, $\sigma_p$ | MWCO* (kDa) (Pore Size Corresponding to MWCO†) |
|---|---|---|---|---|---|
| A | Unmodified | 88.4 | 9.0 | 2.2 | 100.8 (20.5 nm) |
| A (−) | Sulfonated | 57.3 | 5.7 | 1.9 | 57.8 (15.0 nm) |
| B | Unmodified | 157.4 | 5.2 | 2.1 | 44.8 (13.1 nm) |
| B(−) | Sulfonated | 95.1 | 2.9 | 1.9 | 13.7 (6.7 nm) |
| C | Unmodified | 53.6 | 3.5 | 2.0 | 21.5 (8.7 nm) |
| C(−) | Sulfonated | 44.1 | 2.2 | 1.7 | 6.4 (4.4 nm) |
| D | Unmodified | 87.8 | 4.1 | 1.8 | 18.6 (8.0 nm) |
| D(−) | Sulfonated | 44.0 | 2.2 | 1.7 | 6.9 (4.6 nm) |
| D(+) | Triethylaminated | 42.9 | 3.0 | 1.7 | 10.3 (5.8 nm) |
| E | Unmodified | 42.7 | 4.9 | 1.7 | 25.0 (9.4 nm) |
| E(−) | Sulfonated | 23.9 | 2.3 | 1.7 | 6.6 (4.5 nm) |
| E(+) | Triethylaminated | 31.7 | 2.9 | 1.7 | 10.0 (5.7 nm) |

*MWCO: Molecular weight cutoff, i.e., the molecular weight of a solute, 90 wt % of which can be rejected for a membrane.
†Pore size corresponding to MWCO: The diameter of a solute, 90 wt % of which can be rejected for a membrane.

a rejection of 50%), geometric standard deviation (the ratio of geometric mean diameters of two solutes with a rejection of 84.13 and 50%, respectively), and MW cutoff (MWCO, the MW of a solute with a rejection of 90%) are summarized in Table 2. Their probability density function curves generated from the parameters in Table 2 are illustrated in the right column of Figure 3. An evident conclusion can be drawn that the fibers with the smaller pore size display the higher protein separation performance. It is speculated that the difference in three-dimensional shapes of BSA and Hb may be a reason to explain why as-spun dual-layer hollow fibers developed in this work show a selective ability for the BSA–Hb mixture only via size-exclusion even though their MWs are very similar.

It is well known that the three-dimensional sizes of BSA and Hb are 14 nm × 4 nm × 4 nm and 7 nm × 5.5 nm × 5.5 nm, respectively.[33] Therefore, the pores with different sizes may cause the different effects on the transport of BSA and Hb through the membranes. When the pore has a size of smaller than 4 nm (type I), it highly restrains both BSA and Hb from passing, and hence shows a nonselective quality. When the pore has sizes between 4 and 5.5 nm (type II), it may completely constrain Hb transport from three directions, whereas for BSA transport, only one direction is restricted, thus leading to a selectivity (i.e., BSA more permeable than Hb). When the pore has a size of larger than 5.5 nm (type III), it possibly allows both BSA and Hb to freely pass along two or three directions and accordingly also exhibits a nonselective quality. Although the pores of both type I and type III are nonselective for the BSA–Hb mixture, their effects on the pore of type II are distinct. The presence of the pore of

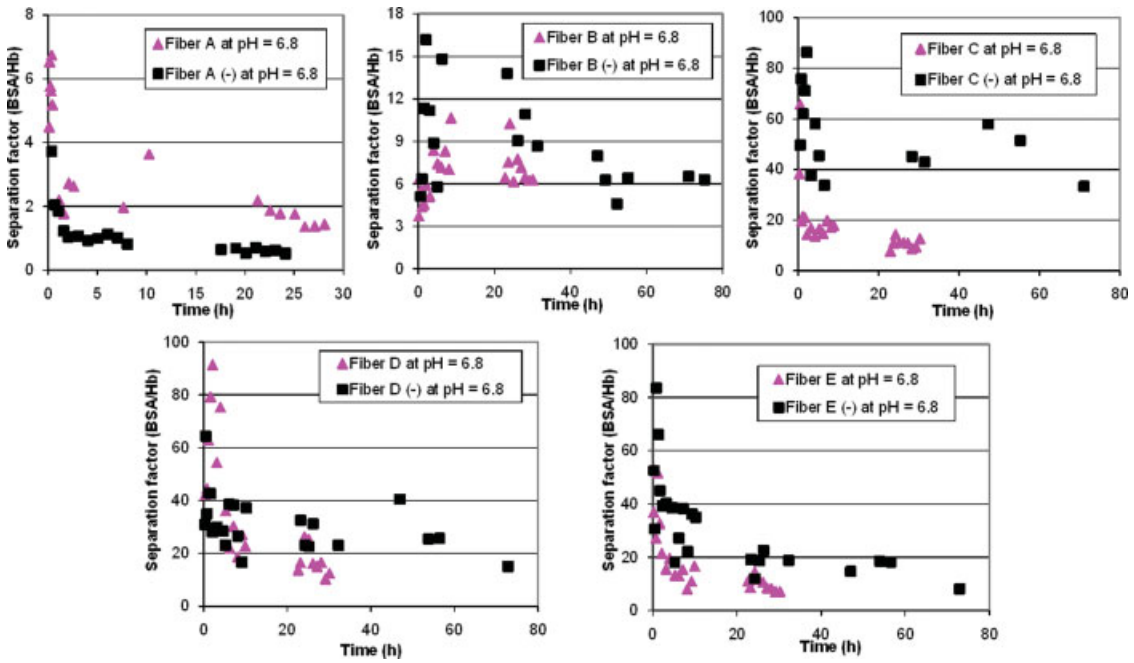


**Figure 4. Comparison of sulfonated hollow fibers with negative charges and as-spun hollow fibers in protein separation performance as a function of time.**

[Color figure can be viewed in the online issue, which is available at www.interscience.wiley.com.]

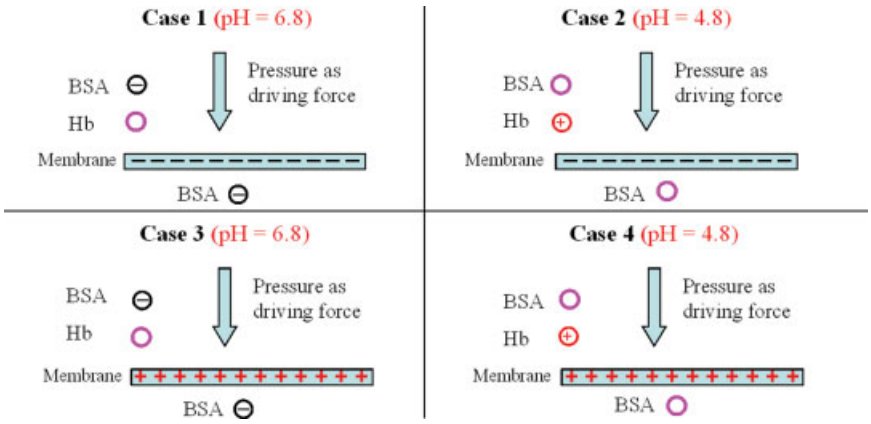


**Figure 5. Schematic of various protein separation environments with two types of membranes (negative or positive charges) and two types of buffers (pH = 6.8 or 4.8).**

[Color figure can be viewed in the online issue, which is available at www.interscience.wiley.com.]

type III may impair the selective function of the pore of type II because both BSA and Hb can pass through the membrane via the pore of type III, whereas the presence of the pore of type I has no influence on the selective ability of the pore of type II. Therefore, the less the proportion of the pores of type III, the higher the BSA/Hb separation factor because more Hb molecules are confined to the retentate side of membranes. This is the reason why fiber D exhibits the best protein separation performance among five kinds of as-spun dual-layer hollow fibers.

### *Protein separation performance of dual-layer hollow fiber membranes with negative charges*

To prove the aforementioned speculation, the sulfonated hollow fibers with negative charges were tested in the BSA–Hb mixture at the same experimental conditions (e.g. pH = 6.8). A comparison of sulfonated fibers with a charge density of 5.0 $\mu$mol/cm$^2$ determined by ion-exchange titration and as-spun fibers in protein separation performance as a function of time is illustrated in Figure 4. It can be seen that all sulfonated fibers with negative charges except fiber A generally exhibit a higher and more durable protein separation performance compared with their corresponding as-spun fibers. This change seems to be contrary to the intuition. When BSA carries negative charges and Hb is neutral at pH = 6.8, the sulfonated fibers with negative charges should reduce the transport of BSA because of electrostatic repulsion as shown in Case 1 of Figure 5, and thus result in a lower BSA/Hb separation performance. The information on the pore size and pore size distribution summarized in Table 2 and Figure 6 may offer a clue to explore the mechanism behind this phenomenon.

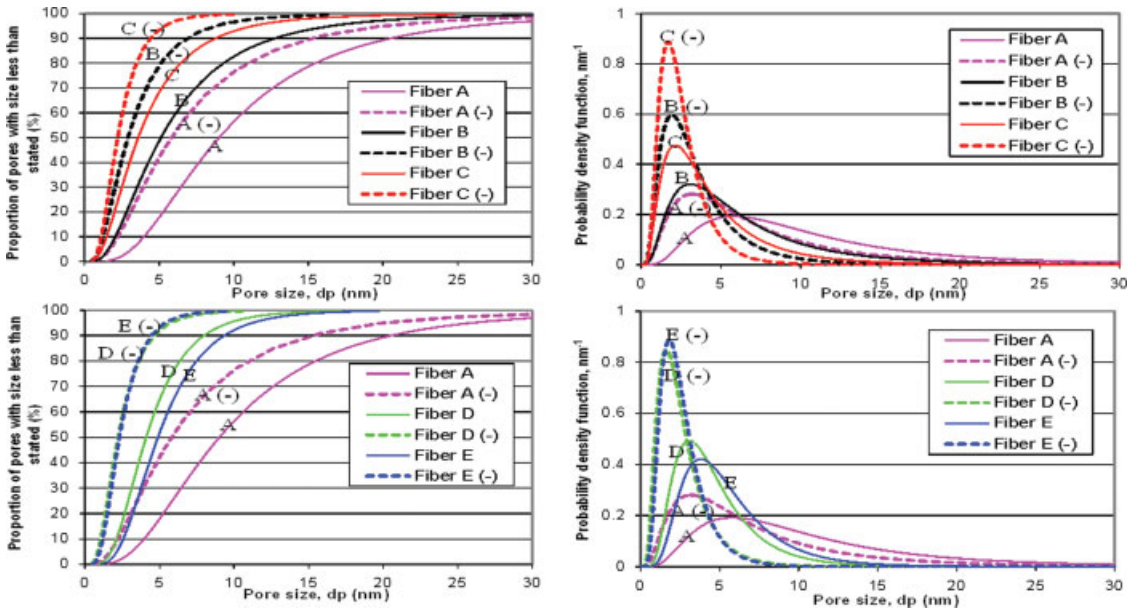


**Figure 6. Comparison of sulfonated fibers with negative charges and as-spun fibers in cumulative pore size distribution (left column) and probability density function curves (right column).**

[Color figure can be viewed in the online issue, which is available at www.interscience.wiley.com.]

**Table 3. Comparison of Various Parameters of Different Dual-Layer Hollow Fiber Membranes on the Protein Sieving Coefficient and the Reduction in Solution Permeation Flux**

| Fiber ID | pH of Buffer | BSA Sieving Coefficient (%) $C_{BSA\ at\ permeate}/C_{BSA\ at\ feed}$ | Hb Sieving Coefficient (%) $C_{Hb\ at\ permeate}/C_{Hb\ at\ feed}$ | Time Needed for the Decrease in Solution Permeation Flux to 50% of its Original Flux |
|---|---|---|---|---|
| A | 6.8 | 22.0–36.2 | 7.2–14.0 | 26 h |
| A(−) | 6.8 | 11.8–18.4 | 4.8–8.9 | 36 h* |
| B | 6.8 | 18.4–30.4 | 3.0–5.0 | 12 h |
| B(−) | 6.8 | 8.8–21.0 | 1.2–2.0 | 24 h |
| C | 6.8 | 12.2–18.9 | 0.4–1.3 | 9 h |
| C(−) | 6.8 | 8.5–13.7 | 0.2–0.4 | 24 h |
| D | 6.8 | 11.1–19.4 | 0.2–1.1 | 40 h* |
| D(−) | 6.8 | 4.4–8.8 | 0.2–0.4 | 48 h |
| D(+) | 6.8 | 1.1–6.4 | 0.2–0.8 | 30 h |
| D(+) | 4.8 | 15.0–33.6 | 0.2–0.4 | 80 h |
| E | 6.8 | 13.1–21.4 | 0.4–2.0 | 40 h* |
| E(−) | 6.8 | 6.7–10.4 | 0.2–0.4 | 48 h |
| E(+) | 6.8 | 1.8–6.8 | 0.4–1.7 | 24 h |
| E(+) | 4.8 | 16.4–33.8 | 0.2–0.4 | 90 h |

*The time was estimated by prolonging the profile of solution permeation flux with time because the solution permeation flux of these three fibers did not decrease to 50% of its original flux during the whole experimental operation.

It can be seen that the pore size of all fibers becomes smaller and their pore size distribution narrows after sulfonation. For example, the pore size of fiber C corresponding to its MWCO is reduced from 8.7 to 4.4 nm after sulfonation as shown in Table 2. Moreover, the cumulative pore size distribution curves of Figure 6 suggest that the proportion of pores of fiber C belonging to type III (i.e., size larger than 5.5 nm and possible Hb permeation channels) is reduced from 26 to 4% (6.5 times) after sulfonation, whereas the proportion of its pores with sizes larger than 4 nm (i.e., possible BSA permeation channels) is diminished from 44 to 14% (3.1 times) after sulfonation. Therefore, higher protein separation performance achieved via sulfonation is due to the fact that the extent of reduction in Hb sieving coefficient induced by the decrease in pore sizes may be higher than that in BSA sieving coefficient resulting from both the decrease in pore sizes and electrostatic repulsion. This speculation is validated by the parameters on the protein sieving coefficient summarized in Table 3. For example, the BSA sieving coefficient of fiber C decreases 1.4 times after sulfonation, whereas its Hb sieving coefficient diminishes 2–3 times after sulfonation. Therefore, these results indicate that size-exclusion is still a dominant factor for improved BSA/Hb separation factor even though the electrostatic interaction in Case 1 results in an adverse effect on BSA/Hb separation.

As shown in Figure 4, fiber A exhibits an opposite trend to other four types of fibers; namely, sulfonated fiber A with negative charges reveals a lower protein separation performance than as-spun fiber A. It can be calculated from the cumulative pore size distribution curves of Figure 6 that after sulfonation, the possible permeation channels of fiber A for Hb and BSA transport only decrease 1.4 and 1.3 times, respectively, because of its relatively large pore size in this study. As a result, the difference in the extent of reduction in Hb and BSA permeation channels is so small that it may not offset the negative effect induced by electrostatic repulsion on BSA transport. Therefore, it can be seen in Table 3 that the BSA sieving coefficient of fiber A decreases 1.9 times because of a combining effect of pore size reduction and electrostatic repulsion, whereas its Hb sieving coefficient lessens 1.5 times because of the reduction in pore sizes.

Another advantage which can be noted in Figure 4 is that sulfonated hollow fibers with negative charges display a more durable protein separation performance than their corresponding as-spun fibers. This may be due to the fact that the membranes become more hydrophilic after sulfonation,[28] thereby significantly reducing membrane fouling and prolonging the longevity of membrane service. This conjecture is possibly supported by the results in Table 3, wherein the time needed for the decrease in solution permeation flux to 50% of its original flux becomes longer after sulfonation.

### *Protein separation performance of dual-layer hollow fiber membranes with positive charges*

Although the protein separation performance of hollow fibers developed in this work is improved via sulfonation, it is not very desirable for industrial applications because of its relatively low BSA concentration at the permeate side of membranes. Therefore, Cases 3 and 4 shown in Figure 5 are applied to augment the BSA concentration at the permeate side of membranes by introducing electrostatic attraction in Case 3 (i.e., positive membranes at pH = 6.8) or eliminating electrostatic repulsion in Case 4 (i.e., positive membranes at pH = 4.8) for BSA transport.

It can be seen in both Table 2 and left column of Figure 7 that the pore sizes of positive fibers D and E via triethylamination are between their as-spun and negative counterparts. Therefore, for Case 3 (i.e., pH = 6.8), the Hb sieving coefficients of positive fibers D and E are between their as-spun and negative counterparts as shown in Table 3 because of the absence of electrostatic interaction for Hb transport. However, the BSA sieving coefficients of positive fibers D and E show a lowest value at pH = 6.8. This seems to be contrary to the intuition because electrostatic attraction between positive membranes and negative BSA is expected to enhance the BSA sieving coefficient. After deliberation, a possible reason is proposed that the flexuosity and complexity of membrane pores make it very difficult to push those

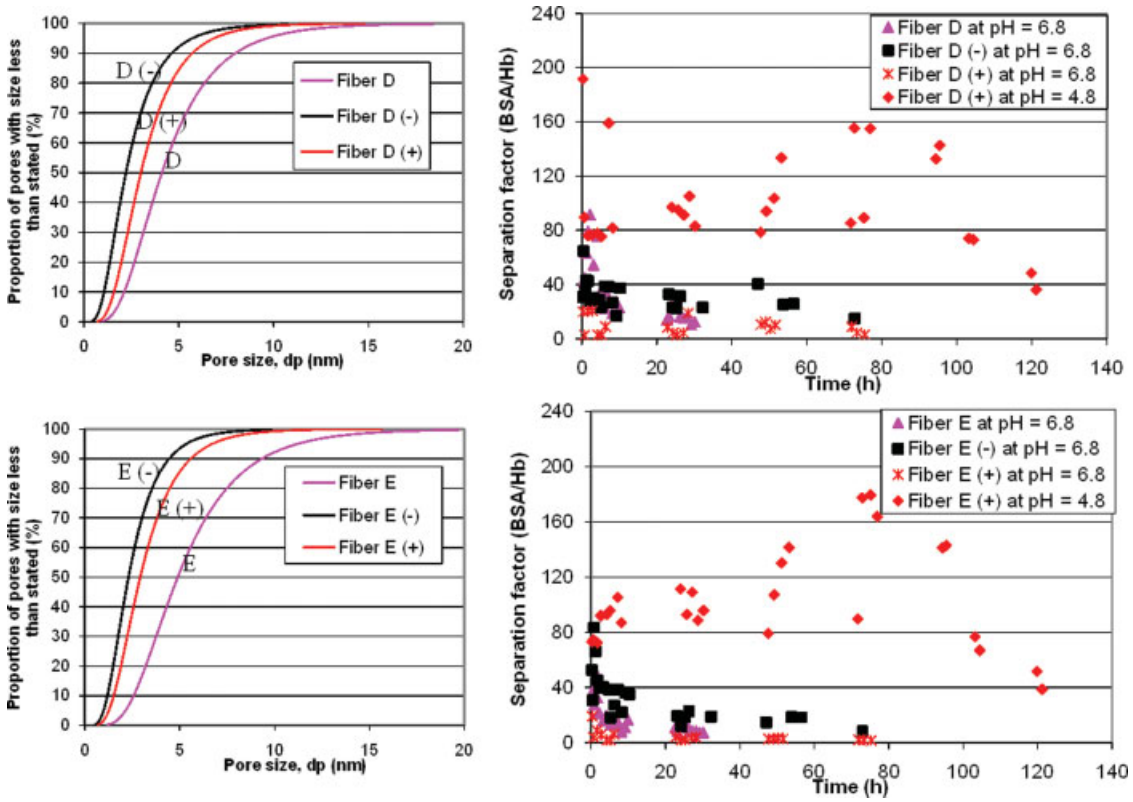


**Figure 7. Comparison of effects of different ionic modification methods on cumulative pore size distribution (left column) and protein separation performance (right column) of fibers D and E.**

[Color figure can be viewed in the online issue, which is available at www.interscience.wiley.com.]

BSA molecules trapped on the membrane pore wall via electrostatic attraction out of the membranes. Namely, a part of BSA molecules may be retained in the membrane, thus leading to a lowest BSA concentration at the permeate side of membranes. This also probably explains why the positive fibers D and E reveal a faster reduction in solution permeation flux in Case 3 (i.e., pH = 6.8) compared with their as-spun and negative counterparts as shown in Table 3. Consequently, it is easily understandable that these positive fibers exhibit a poorest BSA/Hb separation performance at pH = 6.8 as shown in the right column of Figure 7.

On the other hand, although the pore sizes of positive fibers D and E by triethylamination are larger than those of their negative counterparts in Table 2 and Figure 7, their Hb sieving coefficients at pH = 4.8 (Case 4) are as low as those of negative counterparts shown in Table 3 because of the effect of electrostatic repulsion on Hb transport. Meanwhile, the BSA sieving coefficients of positive fibers D and E at pH = 4.8 are significantly enhanced compared with their negative counterparts because of the larger pore size and the absence of electrostatic repulsion for BSA transport, wherein the maximum is 33% shown in Table 3. Therefore, a long-term high-performance protein separation is achieved by applying positive fibers D and E at pH = 4.8, wherein their BSA/Hb separation factor is maintained above 80 for 4 days as shown in Figure 7. These results demonstrate that the ionic modification with the aid of dual-layer hollow fiber technology is an effective approach to produce high-purity and high-concentration protein solutions by fine tuning the pore size and pore size distribution, introducing the electrostatic interaction, and reducing membrane fouling.

## Conclusions

The following conclusions can be drawn from this work:

(1) Both SEM images and results of neutral solute permeation experiments prove that for as-spun hollow fibers, the less the proportion of the pores with sizes larger than 5.5 nm, the higher the BSA/Hb separation factor because more Hb molecules may be confined to the retentate side of membranes. Therefore, the sequence of protein separation performance at pH = 6.8 is fiber C > fiber B > fiber A with the effect of take-up rates and fiber D > fiber E > fiber A with the effect of air gaps.

(2) All negative fibers via sulfonation except fiber A generally exhibit a higher and more durable BSA/Hb separation performance at pH = 6.8 than their as-spun fibers. This is due to the fact that the extent of reduction in Hb sieving coefficient caused by the decrease in pore sizes after sulfonation may be higher than that in BSA sieving coefficient resulting from both the decrease in pore sizes and electrostatic repulsion, and moreover, higher hydrophilicity via sulfonation probably reduces membrane fouling and prolongs its longevity.

(3) When the positive fibers by triethylamination are applied at pH = 6.8, a poorest BSA/Hb separation performance

is revealed because a part of BSA molecules are possibly trapped on the membrane pore wall via electrostatic attraction between positive membranes and negative BSA and, thus, may not pass through the membrane. However, when these positive fibers are used at pH = 4.8, a long-term high-performance protein separation is achieved, wherein their BSA/Hb separation factor is maintained above 80 for 4 days. This is because the Hb sieving coefficient is restrained and, meanwhile, the BSA sieving coefficient is enhanced under this condition, which is attractive for the industrial production of high-purity and high-concentration protein solution.

## Acknowledgments

The authors appreciate A*STAR and NUS for funding this research via grant numbers R-279-000-164-305 and R-279-000-249-646. They thank Solvay Advanced Polymers L.L.C for providing the PES polymer.

## Literature Cited

1. Fersht A. *Structure and Mechanism in Protein Science*. New York: W.H. Freeman and Company, 1999.
2. Creighton TE. *Protein*, 2nd ed. New York: W.H. Freeman and Company, 1993.
3. Feins M, Sirkar KK. Highly selective membranes in protein ultrafiltration. *Biotechnol Bioeng*. 2004;86:603–611.
4. Shah A. Separation systems for commercial biotechnology. Report ID: BIO011D. Published Feb 1, 2007. BCC Research, 2007.
5. Kurnik RT, Yu AW, Blank GS, Burton AR, Smith D, Athalye AM, van Reis R. Buffer exchange using size exclusion chromatography, countercurrent dialysis, and tangential flow filtration: models, development, and industrial application. *Biotechnol Bioeng*. 1995;45:149–157.
6. Christy C, Vermant S. The state-of-the-art of filtration in recovery processes for biopharmaceutical production. *Desalination*. 2002;147:1–4.
7. Cherkasov AN, Polotsky AE. The resolving power of ultrafiltration. *J Membr Sci*. 1996;110:79–82.
8. Saksena S, Zydney AL. Effect of solution pH and ionic strength on the separation of albumin from immunoglobulins (IgG) by selective filtration. *Biotechnol Bioeng*. 1994;43:960–968.
9. van Reis R, Brake JM, Charkoudian J, Burns DB, Zydney AL. High-performance tangential flow filtration using charged membranes. *J Membr Sci*. 1999;159:133–142.
10. Higuchi A, Ishada Y, Nakagawa T. Surface modified polysulfone membranes: separation of mixed proteins and optical resolution of tryptophan. *Desalination*. 1993;90:127–136.
11. Rao S, Zydney AL. High resolution protein separations using affinity ultrafiltration with small charged ligands. *J Membr Sci*. 2006;280:781–789.
12. Burns DB, Zydney AL. Contributions to electrostatic interactions on protein transport in membrane system. *AIChE J*. 2001;47:1101–1114.
13. Ho CC, Zydney AL. Transmembrane pressure profiles during constant flux microfiltration of bovine serum albumin. *J Membr Sci*. 2002;209:363–377.
14. Kim KJ, Sun P, Chen V, Wiley DE, Fane AG. The cleaning of ultrafiltration membranes fouled by protein. *J Membr Sci*. 1993;80:241–249.
15. Munoz-Aguado MJ, Wiley DE, Fane AG. Enzymatic and detergent cleaning of a polysulfone ultrafiltration membrane fouled with BSA and whey. *J Membr Sci*. 1996;117:175–187.
16. Chan R, Chen V, Bucknall MP. Quantitative analysis of membrane fouling by protein mixtures using MALDI-MS. *Biotechnol Bioeng*. 2004;85:190–201.
17. Lee JH, Ju YM, Kim DM. Platelet adhesion onto segmented polyurethane film surfaces modified by addition and crosslinking of PEO-containing block copolymers. *Biomaterials*. 2000;21:683–691.
18. Bhat RR, Chaney BN, Rowley J, Vinson AL, Genzer J. Tailoring cell adhesion using surface-grafted polymer gradient assemblies. *Adv Mater*. 2005;17:2802–2807.
19. Sharma S, Popat KC, Desai TA. Controlling nonspecific protein interactions in silicon biomicrosystems with nanostructured poly(ethylene glycol) films. *Langmuir*. 2002;18:8728–8731.
20. Li DF, Chung TS, Wang R, Liu Y. Fabrication of fluoropolyimide/polyethersulfone (PES) dual-layer asymmetric hollow fiber membranes for gas separation. *J Membr Sci*. 2002;198:211–223.
21. Jiang LY, Chung TS, Li DF, Cao C, Kulprathipanja S. Fabrication of matrimid/polyethersulfone dual-layer hollow fiber membranes for gas separation. *J Membr Sci*. 2004;240:91–103.
22. Li Y, Cao C, Chung TS, Pramoda KP. Fabrication of dual-layer polyethersulfone (PES) hollow fiber membranes with an ultrathin dense selective layer for gas separation. *J Membr Sci*. 2004;245:53–60.
23. Yang MC, Lin WC. Ultrafiltration of myoglobin using surface-sulfonated polysulfone hollow fiber. *J Polym Res*. 2002;9:61–67.
24. Li DF, Chung TS, Wang R. Morphological aspects and structure control of dual-layer asymmetric hollow fiber membranes formed by a simultaneous co-extrusion approach. *J Membr Sci*. 2004;243:155–175.
25. Wang KY, Matsuura T, Chung TS, Guo WF. The effects of flow angle and shear rate within the spinneret on the separation performance of poly(ethersulfone) (PES) ultrafiltration hollow fiber membranes. *J Membr Sci*. 2004;240:67–79.
26. Wang KY, Chung TS. The characterization of flat composite nanofiltration membranes and their applications in the separation of cephalexin. *J Membr Sci*. 2005;247:37–50.
27. Musale DA, Kulkarni SS. Relative rates of protein transmission through poly(acrylonitrile) based ultrafiltration membranes. *J Membr Sci*. 1997;136:13–23.
28. Li Y, Chung TS. Exploration of highly sulfonated polyethersulfone (SPES) as a membrane material with the aid of dual-layer hollow fiber fabrication technology for protein separation. *J Membr Sci*. 2008;309:45–55.
29. Li Y, Chung TS, Chan SY. High-affinity sulfonated materials with transition metal counterions for enhanced protein separation in dual-layer hollow fiber membrane chromatography. *J Chromatogr A*. 2008;1187:285–288.
30. Qin JJ, Gu J, Chung TS. Effect of wet and dry-jet wet spinning on the shear-induced orientation during the formation of ultrafiltration hollow fiber membranes. *J Membr Sci*. 2001;182:57–75.
31. Chung TS. The limitations of using Flory-Huggins equation for the states of solutions during asymmetric hollow fiber formation. *J Membr Sci*. 1997;126:19–34.
32. Qin JJ, Oo MH, Li Y. Hollow fiber ultrafiltration membranes with enhanced flux for humic acid removal. *J Membr Sci*. 2005;247:119–125.
33. Shukla R, Balakrishnan M, Agarwal GP. Bovine serum albumin-hemoglobin fractionation: significance of ultrafiltration system and feed solution characteristics. *Bioseparation*. 2000;9:7–19.

*Manuscript received May 19, 2008, and revision received Aug. 16, 2008.*